

Research article

# Improvement of the drug encapsulation into biodegradable polyester nanocarriers by blending of poly(lactic-co-glycolic acid) and polycaprolactone

Ágnes Ábrahám<sup>1,2\*</sup>, Gergő Gyulai<sup>1</sup>, Tünde Tóth<sup>1</sup>, Barna Szvoboda<sup>1</sup>, Judith Mihály<sup>3</sup>, Ákos Szabó<sup>4</sup>, Éva Kiss<sup>1</sup>

<sup>1</sup>Laboratory of Interfaces and Nanostructures, Institute of Chemistry, Eötvös Loránd University, H-1518 Budapest 112 PO Box 32

<sup>2</sup>MTA-ELTE Lendület ‘Momentum’ Peptide-based Vaccines Research Group, Eötvös Loránd University, Pázmány Péter sétány 1/a, H-1117 Budapest, Hungary

<sup>3</sup>Biological Nanochemistry Research Group, Institute of Materials and Environmental Chemistry, Research Centre for Natural Sciences, H-1117 Budapest, Magyar tudósok körútja 2, Hungary

<sup>4</sup>Polymer Chemistry Research Group, Institute of Materials and Environmental Chemistry, Research Centre for Natural Sciences, H-1117 Budapest, Magyar tudósok körútja 2, Hungary

Received 12 February 2022; accepted in revised form 15 May 2022

**Abstract.** Biocompatible and biodegradable polymers such as poly(lactic-co-glycolic acid), PLGA and polycaprolactone, PCL nanoparticles (NPs) have been used successfully as drug carriers in controlled drug release. The main weakness is the generally low drug loading (1–5%) of the NPs. An option to enhance the drug content of NPs is to find the optimum matrix for a given drug molecule. To reveal the influence of matrix and drug polarity on the favoured encapsulation, polymeric NPs loaded with a series of alkyl-4-hydroxybenzoate (paraben) with increasing alkyl chain length (C1–C8) as model drugs were prepared by nanoprecipitation method. The paraben series represents the drugs with various polarities while the selected matrix polymers show increased hydrophobicity: PLGA with 50% lactic acid content (PLGA50) < PLGA with 75% lactic acid content (PLGA75) < PCL. The drug content of the PLGA NPs was found to significantly increase up to 10% with the hydrophobicity of the parabens, while encapsulation was further boosted by applying PCL. To find the proper fit between drug and matrix and finely tune the polarity of the NPs, as a novel approach, blends of PLGA50 and PCL were applied as matrix polymers. The drug loading of the NPs was proved to be dependent on the systematically changed blend composition. Furthermore, the introduction of PCL into the PLGA50 matrix improves the release kinetics of the active component.

**Keywords:** biocompatible polymers, controlled drug delivery, polycaprolactone, poly(lactic-co-glycolic acid), blended polymeric nanoparticles

## 1. Introduction

Novel drug delivery systems play a crucial role in disease treatment and are gaining increasing importance. The development and application of these systems can improve the bioavailability and therapeutic efficacy of the drug while resulting in reduced side effects. Several systems have already been utilized

for this purpose, such as liposomes, cyclodextrins, nanoparticles [1–5] or nanofibres [6–8].

Nanoencapsulation of an active ingredient (drugs, vitamins *etc.*) within a secondary material as a matrix or shell is a promising method for the development of nanomedicines [9]. The core contains the active component while the shell protects it from the

\*Corresponding author, e-mail: [abraham.agnes@ttk.elte.hu](mailto:abraham.agnes@ttk.elte.hu)

© BME-PT

surrounding environment. The drug is released by diffusion or in response to a trigger (pH, enzyme reaction etc.), enabling the controlled and prolonged delivery in the body.

Polymeric nanoparticles (nanospheres) are those systems in which the drug is homogeneously dispersed within the polymer matrix [10]. They provide a convenient way for drug delivery, facilitating various administration routes such as oral, nasal, intravenous, percutaneous [11], while enabling the dispersion of hardly soluble active compounds.

The FDA-approved polyesters (PLGA, PLA, PGA and PCL) are the most widely used polymers for nanocarrier preparation. The biodegradable and biocompatible carriers formed from these polyesters using the nanoprecipitation technique results in delivery systems with narrow particle size distribution in the diameter range of a few hundred nanometers. The molecular weight, composition, stereoregularity, the polarity of polyesters as well as preparation conditions all influence the physico-chemical, and pharmaceutical properties of the drug-loaded NP system [12–19]. Since the mechanism of drug release usually involves the swelling and erosion of the polymer matrix, its composition is a crucial factor influencing the drug release kinetics. PLGA and PLA are the most widely used polyesters used for nanoparticle preparation. PCL is mostly used as a fibrous system for wound healing and tissue engineering [20–23] due to its good mechanical properties, stability and hydrophobic character. Its application as a colloidal drug carrier is less common [24–27]. Due to their particular size properties, NPs can be administered by the parenteral route and can gain access to tissues beyond the capillary blood supply. They are especially suitable to achieve temporal and site-specific delivery. The targeting of specific organs or cells might highly enhance the efficacy of therapy [28, 29].

Nanoprecipitation as a technique for NP preparation has substantial benefits [30], such as being a rapid method with high reproducibility, good stability and being easy to scale-up. However, its main limitation is the low encapsulation efficiency and that the drug content of the polymeric nanoparticles hardly exceeds 1–5% [12, 16, 31, 32].

Most reports on NP drug carrier preparation are dealing with one specific therapeutic to optimize its encapsulation. Our aim was to get a wider overview of the influence of drug and matrix polarity on the entrapment efficiency into polyester drug carriers.

As model drugs parabens, a homologous series of an organic molecule were selected. Parabens are alkyl esters of p-hydroxybenzoic acid and are used as preservatives [33]. Their antimicrobial effectiveness is correlated with the ester substituent in the homologous series (increasing with increasing alkyl chain length) [34]. This is an ideal molecular family to study the gradually changing hydrophobic character with increasing alkyl chain length while the character of the chemical structure is the same. With the purpose of revealing how the chemical composition and hence the polarity of both the drug and the matrix polymers influenced their interactions leading to drug encapsulation, various polyesters, PLGA50, PLGA75, PCL were used for NP preparation. A series of parabens with increasing alkyl chain length from methyl to octyl were entrapped into the various polymer NPs by nanoprecipitation method.

Furthermore, as a novel approach for the tuning of matrix polarity PLGA50 and PCL were blended for the drug nanoencapsulation. The effect of the systematically changed ratio of the PLGA50 and PCL components in the blend NPs on the drug content of two selected parabens, a less- and a more hydrophobic butyl- and hexylparabens, respectively, was evaluated. The release kinetics were analysed and compared using various models.

## 2. Experimental

### 2.1. Materials

Poly(D,L-lactic-co-glycolic acid), PLGA, with different ratios of lactic and glycolic acid content (50% of lactic acid content ( $M_w$ : 38 000–54 000 g/mol), PLGA50); 75% of lactic acid content ( $M_w$ : 90 000–126 000 g/mol), PLGA75), poly( $\epsilon$ -caprolactone), PCL, with a molecular weight of 45 000 g/mol were purchased from Sigma-Aldrich Kft., Hungary. Poly(ethylene oxide)/poly(propylene oxide)/poly(ethylene oxide) PEO/PPO/PEO triblock copolymer, Pluronic F 127 ( $M_w$ : 12 700 g/mol), was provided by BASF Hungaria Kft, Hungary.

Alkyl-4-hydroxybenzoates (Sigma-Aldrich Kft., Hungary) (parabens) with increasing alkyl chain length as model drugs were loaded into polymer NPs. Their main properties are collected in Table 1.

Tetrahydrofuran (THF) (for HPLC, purity  $\geq$  99%, VWR International Kft., Hungary), THF was used in the preparation of the nanoparticles and as a solvent in the drug content determination.

**Table 1.** Main parameters of the encapsulated compounds, alkyl-4-hydroxybenzoates: alkyl chain length, molecular weight ( $M_w$ ), aqueous solubility at 25 °C ( $S$ ) and partition coefficient between n-octanol and water ( $\log P_{\text{oct/w}}$ ).

Paraben	$M_w$ [g/mol]	$S$ [g/l]	$\log P_{\text{oct/w}}^a$ [–]
Methyl	152.1	2.500	1.96
Ethyl	166.2	0.885	2.47
Propyl	180.2	0.500	3.04
Butyl	194.2	0.207	3.57
Pentyl	208.3	0.032	3.92
Hexyl	222.3	0.025	4.30
Heptyl	236.3	0.020	4.83
Octyl	250.3	0.015	5.43

<sup>a</sup>experimental values [35]

Ethanol (for HPLC, purity  $\geq 99\%$ , VWR International Kft., Hungary) in 50 v% aqueous solution was used as a medium during the drug release measurements.

Doubled distilled water was checked by its conductivity ( $<5$  mS) and surface tension ( $>72.0$  mN/m at  $(23.0 \pm 0.5)$  °C).

## 2.2. Methods

### 2.2.1. Preparation and characterization of the drug-loaded polymer nanoparticles

PLGA and PCL NPs were prepared by the nanoprecipitation method. Briefly, PLGA or PCL was dissolved in THF to a concentration of 10 g/l. For drug encapsulation, 5 mg paraben was dissolved in 1 ml PLGA or PCL solution. This organic solution was added dropwise to 10 ml aqueous solution of the stabilizer, Pluronic F 127 (1 g/l) under magnetic stirring (500 rpm) to form NPs. The stirring was continued in a fume hood overnight to achieve the complete evaporation of THF. The sample was centrifuged at 3000 rpm for 10 min to remove possible polymer aggregates and unloaded undissolved drugs. The supernatant, containing the NPs and unloaded, but dissolved drugs, was separated and further purified from the Pluronic F 127 stabilizer excess and unloaded drugs by centrifugation at 14 500 rpm for 20 min. The supernatant containing the unloaded drugs and excess stabilizer was discarded, and the pellet containing the particles was redispersed with double distilled water. This step was repeated three times. The supernatants were checked for drug content using UV-Vis spectroscopy. After the second centrifugation, drug content in the particle medium was below

**Table 2.** Composition of polymers used for butyl- and hexyl-paraben nanoencapsulation.

NP system	Polymer composition	
	PLGA50	PCL
	$\text{HO} \left[ \text{CH} \left( \text{CH}_3 \right) \text{C} \left( \text{O} \right) \right]_n \left[ \text{CH}_2 \text{C} \left( \text{O} \right) \right]_m \text{H}$ $[w\%]^a$	$\left[ \text{O} \left( \text{CH}_2 \right)_6 \text{C} \left( \text{O} \right) \right]_k$ $[w\%]^b$
1	100	0
2	80	20
3	60	40
4	40	60
5	20	80
6	0	100

<sup>a</sup> $n$  and  $m$  indicate the ratio of the lactic acid and the glycolic acid content of the polymer, in the case of PLGA50  $n, m = 50$

<sup>b</sup> $k$  is the monomer unit

detection limits. The final nanoparticle yield was about 50–60%.

For encapsulation into the blend of PLGA50 and PCL, butyl- (B) and hexylparabens (H) were selected. The composition of the polymer for NP preparation is shown in Table 2. The drug-free, the butyl-paraben, and the hexylparaben containing NP systems are indicated by N, B and H, respectively.

Measured data present the mean with standard deviations of three determinations on parallel samples in the various characterization of NPs.

The average hydrodynamic radius and the polydispersity of the NPs were determined using dynamic light scattering (DLS) equipment based on 3D modulation technology (NanoLab 3D, LS Instruments, Switzerland). As a light source, a fibre-coupled diode laser operating at 638 nm was used. The measurements were performed at a detection angle of 90° at  $(25.00 \pm 0.02)$  °C. The measured autocorrelation functions were analysed by the second-order cumulant expansion method.

The electrophoretic mobility of the nanoparticles was determined by Laser Doppler-electrophoresis Malvern Zetasizer 4 apparatus (Malvern Panalytical Ltd., United Kingdom) at  $(25 \pm 1)$  °C. Smoluchowski approximation was used to calculate zeta potential from mobility values.

### 2.2.2. Determination of the drug content of the polymer nanoparticles

An aliquot of the NP suspension was dried at 55 °C under reduced pressure to obtain the mass of the nanoparticles and then these dried nanoparticles were dissolved in THF. Spectrophotometric measurements

were taken with a Specord 40 UV-VIS spectrophotometer (Analytik Jena AG, Germany). The absorption spectra of this solution were recorded in 1.0 cm quartz cell over the 200–250 nm wavelength range at room temperature. The drug concentration was calculated using the absorbance – drug concentration calibration curve determined at the wavelength of maximum absorbance of the respective paraben. The drug content (DC) was provided by Equation (1):

$$DC = \frac{\text{mass of drug in the NPs}}{\text{mass of the NPs}} \cdot 100\% \quad (1)$$

### 2.2.3. Solubility parameter calculation

The solubility parameters for the parabens were calculated by group contribution methods [36–39]. These approaches are based on the theory that the cohesive energy density of a molecule is an additive property and it can be derived as the sum of contributions from the individual functional groups within the molecule.

According to an extension of Hildebrand's concept, dividing this energy by the molar volume gives the square of the total solubility parameter as the sum of the squares of the partial solubility parameters (Equation (2)):

$$\delta = \sqrt{\delta_d^2 + \delta_p^2 + \delta_h^2} \quad (2)$$

where  $\delta_d$ ,  $\delta_p$  and  $\delta_h$  partial solubility parameters represent the dispersion, the polar, and the hydrogen bonding interactions.

The Fedors method is a simpler estimation of the total solubility parameter (Equation (3)):

$$\delta = \sqrt{\frac{\Delta E_v}{\Delta V}} \quad (3)$$

where  $\Delta E_v$  represents the energy of vaporization at a given temperature (the substituent fragment constant) and  $\Delta V$  represents the fragmental molar volume constant.

The van Krevelen method determines the total and the partial solubility parameters (Equations (4)–(6)):

$$\delta_d = \frac{\sum F_d}{V} \quad (4)$$

$$\delta_p = \frac{\sqrt{\sum F_p^2}}{\sqrt{\sum V}} \quad (5)$$

$$\delta_h = \frac{\sqrt{\sum E_h}}{\sqrt{\sum V}} \quad (6)$$

$F_d$ ,  $F_p$ ,  $E_h$  are the group contribution to dispersion forces, polar forces and hydrogen bond energy, respectively, and  $V$  is the molar volume.

The Hansen-Bower approach uses other formulations for the  $\delta_p$  estimation (Equation (7)):

$$\delta_p = k_{HB} \frac{\mu}{\sqrt{V}} \quad (7)$$

where  $\mu$  is the dipole momentum of the molecule and  $k_{HB}$  is 37.4.

### 2.2.4. FTIR spectroscopy

Interaction between polymer matrix and parabens was interrogated using attenuated total reflection infrared (ATR-IR) spectroscopy. Collection of IR spectra was performed using a Varian (Scimitar Series) 2000 FT-IR spectrometer (Varian Inc, USA) with broadband MCT detector and fitted with a 'Golden Gate' single reflection diamond ATR accessory (Specac Ltd, UK). 3  $\mu$ l of sample solution was evaporated (under gentle nitrogen flow) onto the surface of the ATR crystal, and spectra were recorded (64 scans and 4  $\text{cm}^{-1}$  spectral resolution) within approx. 5 minutes. All spectral manipulations were made after ATR correction, using the GRAMS/AI (7.02) spectroscopy software package (Thermo Scientific, USA).

### 2.2.5. Differential scanning calorimetry

Differential scanning calorimetry (DSC) measurements were performed on a Mettler DSC821e equipment (Mettler Toledo International Inc. USA) using 0–200 °C temperature interval, 10 °C/min heating/cooling rate and  $\text{N}_2$  atmosphere. First heating and subsequent cooling curves were evaluated and the inflection point temperatures were considered as glass temperatures.

### 2.2.6. Drug release kinetics

The paraben release from the PLGA, PCL and blend nanoparticles were investigated by dialysis method. 5 ml of each sample was transferred into a 3.5–5 kDa regenerated cellulose dialysis bag. The bags were immersed in 50 ml of 50 v% aqueous ethanol solution. The medium was constantly stirred with 300 rpm at (37 $\pm$ 0.5) °C. 1 ml of the medium was taken at given times (10, 20, 30, 40, 50, 60, 90, 120, 180, 240



and 1260 min) while the medium was replaced by fresh solution consecutively. The concentration of paraben was determined by spectrophotometrically as described in the previous section.

Experimental models for describing drug release kinetic provide a means to understand the mechanism of drug release. For our calculations, the following kinetic models were used.

The Gompertz model is a simple exponential model suitable for burst release profiles where the released drug amount converges to a maximum value. The model is described by Equation (8):

$$\frac{c_t}{c_0} = C_{\max} \cdot \exp[-a \cdot e^{b \cdot \log t}] \quad (8)$$

where  $C_{\max}$  is the maximum dissolution of the drug,  $a$  determines the undissolved proportion at time  $t = 1$  and is described as the location parameter, while  $b$  is the shape parameter, describing the dissolution rate [40].

The Korsmeyer-Peppas model can be used for polymeric systems to find out the mechanism of release by fitting the initial part of the release profile (up to 60–70% released drug content) with Equation (9):

$$\frac{c_t}{c_0} = k \cdot t^n \quad (9)$$

where  $c_t$  is the cumulative amount of released drug up to  $t$  time,  $c_0$  is the total drug content,  $k$  is the release rate constant and  $n$  is the release exponent. The value of  $n$  is used to differentiate between release mechanisms [41].

The Peppas-Sahlin model was also be used to approximate the contributions of different mechanisms in the overall release profile:

$$\frac{c_t}{c_0} = k_1 \cdot t^m + k_2 \cdot t^{2m} \quad (10)$$

where  $k_1$  and  $k_2$  are the contributions of the Fickian and case II mechanisms. The constant  $m$  is 0.43 for spherical particles [42].

### 3. Results and discussion

#### 3.1. Nanoencapsulation into PLGA50, PLGA75 and PCL

The nanoencapsulation of various parabens into PLGA50 NPs stabilized by Pluronic F 127 copolymer has been examined in our previous work [43]. In the present work, drug carrier NPs were formed using PLGA50 and two further polyesters, PLGA75

and PCL for the encapsulation of a complete series of model drugs from methyl- to octylparaben. PLGA75 is more hydrophobic compared to PLGA50 due to the higher ratio of the lactic component, while PCL is considered the most hydrophobic one formed from less polar monomers. The aim was to reveal the influence of polarity of both the drug and matrix polymer on the efficacy of nanoencapsulation.

The average hydrodynamic radius and the polydispersity of the particles prepared were collected in Table 3. The polydispersity parameters show that almost all of the studied NP systems have a narrow size distribution (polydispersity < 0.1). The average radius of PLGA50 NPs is around (82±2) nm, while for PLGA75 NPs is higher, 132–137 nm. PCL NPs were found to be even larger (163–174 nm) but still in the nanoparticle size range. That shows that the chemical composition of the polymer notably affects the nanoprecipitation process and the formation of particles. On the other hand, the type of drug encapsulated does not seem to influence much the size of

**Table 3.** Hydrodynamic radius ( $r_H$ ), polydispersity (PD), zeta potential ( $\zeta$ ) and drug content (DC) of the paraben-loaded PLGA50, PLGA75 and PCL nanoparticles.

	Paraben	$r_H$ [nm]	PD [–]	$\zeta$ [mV]	DC [%]
PLGA50	methyl	80±1	0.06	–24±2	0.2±0.01
	ethyl	83±1	0.06	–24±1	0.2±0.01
	propyl	82±1	0.05	–23±1	0.4±0.10
	butyl	82±1	0.07	–23±1	1.4±0.10
	pentyl	82±2	0.05	–24±1	1.9±0.30
	hexyl	84±2	0.07	–23±1	3.1±0.40
	heptyl	83±1	0.11	–22±1	5.9±0.40
	octyl	83±1	0.03	–16±1	10.1±0.10
PLGA75	methyl	132±1	0.07	–22±1	0.4±0.02
	ethyl	133±1	0.08	–21±1	0.3±0.01
	propyl	132±1	0.07	–22±1	0.5±0.05
	butyl	132±1	0.07	–23±1	0.9±0.04
	pentyl	134±1	0.10	–22±1	2.0±0.30
	hexyl	135±1	0.06	–22±1	2.8±0.40
	heptyl	137±1	0.11	–20±1	4.8±0.60
	octyl	134±1	0.11	–19±1	9.1±0.20
PCL	methyl	163±1	0.10	–15±1	0.5±0.01
	ethyl	164±2	0.11	–16±1	0.6±0.08
	propyl	163±2	0.05	–14±1	0.7±0.03
	butyl	163±3	0.10	–14±1	2.6±0.5
	pentyl	166±2	0.09	–14±1	8.1±0.6
	hexyl	167±2	0.09	–13±1	14.8±0.9
	heptyl	174±4	0.15	–12±1	17.3±0.2
	octyl	171±2	0.10	–12±1	25.4±0.5

the nanoparticles. However, the drug-loaded PCL NPs show a slight (approximately 5%) size increase for parabens with higher hydrophobicity.

The zeta-potential and drug content of the nanoparticles are also summarized in Table 3. All of the drug-loaded polymeric NPs show negative zeta-potential in accordance with previous studies [5, 44] originating most likely from the carboxylic end group of the polyester, which contributes to the colloidal stability of the system. The negative zeta potential does not differ markedly for the two PLGAs. Although the values are lower but still in the negative range (12–15 mV) for PCL particles, similarly to the Pluronic F 68, or hyperbranched polyglycerol stabilized PCL NPs reported [27, 45]. Since the surface of the NP is modified by the adsorbed layer of the stabilizing block-copolymer (Pluronic F 127), the charge character of the particles is altered by its shielding effect. The lower zeta-potential of PCL NPs might be caused by the more preferred adsorption of Pluronic on the more hydrophobic polymer surface.

The efficacy of drug encapsulation is indicated by drug content values summarized in Table 3. The drug loading of the polymeric NPs is very low (<1%) for the less hydrophobic parabens with a short alkyl chain. However, with a longer alkyl chain ( $n_C > 3$ ) there is a considerable increase in the drug content of the nanocarrier. The highest amount of encapsulated drug, about 10% was found for the most hydrophobic octylparaben in PLGA50 and also PLGA75. In PCL however, substantially higher drug content was obtained compared to the PLGA NPs in the whole range of model compounds, except the very hydrophilic ones ( $n_C < 4$ ) with high aqueous solubility (Table 3). The difference is remarkable, the achieved increase in drug content is 2 to 3-fold; thus, the amount exceeds 25% for octylparaben in PCL.

The polarity of model drug molecules and its change in the homologous series is clearly shown by their aqueous solubility data collected in Table 1. The n-octanol/water partition coefficients expressing the relative hydrophobicity of the molecules (log*P* values in Table 1) are changing parallel with the aqueous solubility from methyl- to octylparaben as expected. The tendency for higher drug loading with increasing log*P* and decreasing solubility is similar for all of the three polymers, but there is a marked difference between PLGAs and PCL. Considering the chemical composition, PCL is more hydrophobic than

the PLGAs because of the presence of four methylene groups between the ester bonds in the polymer chain. Comparing PLGA50 and PLGA75 a smaller hydrophobicity difference can be predicted due to the higher ratio of lactic acid related to glycolic acid monomers in the polymer.

The polarity relations of polymers are usually represented by solubility parameters. One approach is to calculate the solubility parameters from group contributions. According to that, the solubility parameters are 21.3, 20.3 and 19.3 for PLGA50, PLGA75 and PCL, respectively [46, 47]. The experimental determination, e.g. by swelling measurement is another possibility, the corresponding values are 22.3, 21.7, and 20.4 [47, 48]. Although the values of solubility parameters are not equal when obtained from the two methods, the hydrophobicity order (PLGA50 < PLGA75 < PCL) is the same. The highly increased drug content achieved by encapsulating with PCL indicates that the higher hydrophobicity (lower solubility parameter) of PCL is favourable for the interaction with parabens, especially for the most hydrophobic ones ( $n_C > 4$ ). The lower hydrophobicity of the PLGAs (higher solubility parameters) might be the cause of weaker interaction with parabens, resulting in poor encapsulation. The behaviour of the two PLGAs is similar, the difference in the chemical structure is probably not sufficient to be clearly manifested in their encapsulation capability.

It seems to be reasonable to estimate the possible interaction between drug and polymer leading to successful encapsulation by considering the similarity of their solubility parameters. The solubility parameters for the parabens were calculated using the various methods referred in the paper of Mande *et al.* [36] and collected in Table 4. The smaller difference between the parameters corresponding to drug and polymer would lead to higher drug content of NPs. The main tendency of increasing encapsulation with the hydrophobicity of parabens is supported by this approach since the solubility parameters of the parabens with a longer alkyl chain are approaching the values for polymers. The large difference between the polymers in their ability to encapsulate the drugs, namely the outstanding performance of PCL cannot be explained by the values of solubility parameters. The excellent ability of PCL to incorporate hydrophobic drug molecules is supposedly closely related to the hydrophobic segments of the polymer chain, which might build hydrophobic domains in

**Table 4.** Calculated solubility parameters of the parabens.

Paraben	$\delta_{\text{Fedors}}$ [MPa <sup>1/2</sup> ]	Components of $\delta_{\text{van Kreeven}}$			$\delta_{\text{van Kreeven}}$ [MPa <sup>1/2</sup> ]	$\delta_{\text{H\&B}}$ [MPa <sup>1/2</sup> ]
		$\delta_{\text{d}}$ [MPa <sup>1/2</sup> ]	$\delta_{\text{p}}$ [MPa <sup>1/2</sup> ]	$\delta_{\text{h}}$ [MPa <sup>1/2</sup> ]		
methyl	27.22	20.11	6.22	15.39	26.08	25.20
ethyl	26.22	19.69	5.45	14.41	25.00	24.49
propyl	25.40	19.37	4.85	13.59	24.15	23.90
butyl	24.73	19.11	4.37	12.90	23.47	23.40
pentyl	24.17	18.90	3.97	12.31	22.90	22.98
hexyl	23.69	18.72	3.64	11.79	22.42	22.61
heptyl	23.28	18.57	3.37	11.33	22.01	22.29
octyl	22.92	18.44	3.13	10.92	21.66	22.01

the nanoparticles beneficial for alkyl chain interactions.

### 3.2. Nanoencapsulation into PLGA50 – PCL blends

#### 3.2.1. Drug loading

In view of the noticeable influence of polymer matrix on the efficacy of encapsulation, it is interesting to see whether there is a possibility to finely tune the polarity of the matrix and hence the drug content by blending the polyesters in question. To know the possibility of the formation of polymer blend NPs by nanoprecipitation and their drug loading, the NPs were prepared using PLGA50 and PCL in various weight ratios for encapsulation of two selected drugs, butyl- and hexylparabens.

The size and zeta potential values obtained for the drug-loaded NPs are collected in Table 5. According to the expectation, the size of the drug-loaded NPs is gradually increasing with the PCL content of the

NP matrix (samples 1 to 6) and is significantly larger for hexylparaben-containing systems compared to the butylparaben loaded ones. It is worth emphasizing that the polydispersity indices (PDI) characterizing the width of size distribution are remarkably low values similarly to systems obtained from single polymers (Table 3). The surface charge of particles is the highest for PLGA50 particles (B1 and H1) and is decreasing with PCL content leading to the lowest (but still above –10 mV) value for pure PCL.

This gradual change of properties as a function of polymer composition implies that the character of both polymers is exposed in their blend systems.

The drug content of butylparaben and hexylparaben containing blend NPs is displayed in Figure 1 as a function of the polymer composition. A substantially higher amount of hexylparaben could be incorporated into all kinds of NPs than butylparaben. The drug loading is between 4 and 17% for hexylparaben, while 2–4% for the more polar butylparaben. Within this range, the hexylparaben content is continuously and greatly increasing, presenting a significant difference between the NP compositions examined here. The trend is similar for butylparaben, but the changes are small, with significant differences only between the systems indicated in Figure 1.

It is interesting to note that the hexylparaben content values obtained for blends are between those of pure polymers, and the change is proved to be linear with the composition of the polymer. It suggests that both polymers are involved in the drug encapsulation in an additive way. The reason behind that might be either an ideal mixing or a complete phase separation of PLGA50 and PCL forming the polymer matrix of NPs.

Further investigations such as IR spectroscopy and DSC measurements are performed to get some

**Table 5.** Size ( $r_{\text{H}}$ ) and zeta potential ( $\zeta$ ) of butyl (B)- and hexyl (H)- paraben loaded PLGA50-PCL blend polymeric nanoparticles (Blend composition is given in Table 2.).

NP system	$r_{\text{H}}$ [nm]	PDI [–]	$\zeta$ [mV]
B1	84±1	0.05	–23±0.5
B2	116±2	0.09	–19±0.4
B3	132±2	0.08	–17±0.3
B4	135±1	0.08	–16±0.5
B5	137±1	0.09	–13±0.3
B6	151±1	0.08	–11±0.6
H1	87±1	0.07	–23±0.4
H2	125±2	0.05	–19±0.3
H3	132±2	0.09	–17±0.2
H4	140±2	0.10	–13±0.2
H5	144±1	0.06	–12±0.3
H6	162±2	0.12	–11±0.6

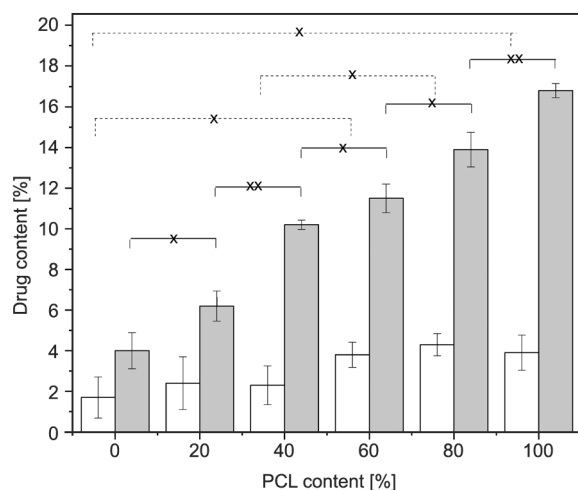


**Figure 1.** Butylparaben (white column) and hexylparaben (grey column) content of various polymer NP systems with increasing PCL ratio in the PLGA50-PCL blend. Statistical significance of the difference obtained by T-test is indicated by x for  $p < 0.05$  and xx for  $p < 0.01$ .

insights into the structure and reveal molecular interactions in the drug-loaded polymeric NPs.

### 3.2.2. IR analysis

IR spectra of butyl- and hexylparaben loaded PLGA50, PCL and two of those blend system NPs as well as of the pure components were collected and comparatively analysed.

Figure 2 shows the IR spectra of pure polymers and those of butyl- and hexylparabens. The spectra of polymers (Figure 2a) are dominated by the strong absorption band of ester bonds ( $\nu_{C=O}$ ,  $\nu_{C-O}$ ). PLGA exhibits a strong carbonyl band at  $1768\text{ cm}^{-1}$ , while

the carbonyl of PCL appears at a lower wavenumber at  $1725\text{ cm}^{-1}$  [27]. In line with the structure of PCL, characteristic bands of  $-\text{CH}_2-$  moieties at  $2946$  and  $2868\text{ cm}^{-1}$  are also visible [49]. As to the polymer mixtures, the spectral features of both PLGA and PCL can be recognized.

The spectra of the two parabens (Figure 2b) are very similar. They differ only in the intensity of the anti-symmetric ( $2932\text{ cm}^{-1}$ ) and symmetric ( $2859\text{ cm}^{-1}$ ) stretching bands of  $\text{CH}_2$  groups, confirming their chemical structure. Determining bands are the band of carbonyl stretching vibration ( $\nu_{C=O}$ ) at  $1683\text{ cm}^{-1}$ , with a shoulder at  $1712\text{ cm}^{-1}$ . The position of  $\nu_{C=O}$  band suggests that a strong H-bonding exists between the  $\text{C=O}$  and  $-\text{OH}$  groups of adjacent paraben molecules, presuming strong intermolecular interactions. Further characteristic bands are the doublet at  $1608$  and  $1591\text{ cm}^{-1}$ , assigned to ring  $\text{C-C}$  stretching vibrations ( $\nu_{C-C}$  ring), and the multiple bands around  $1281\text{ cm}^{-1}$  belonging to  $\text{C-O}$  stretching vibrations ( $\nu_{C-O}$ ) [50].

In the case of paraben-loaded polymer nanoparticles, both the vibration bands corresponding to polymer and that of paraben can be witnessed. Irrespectively of the polymer composition, the amount of loaded hexylparaben exceeds that of loaded butylparaben. Furthermore, detailed spectral analysis performed on difference spectra of loaded polymer NPs (the spectra of the paraben-loaded polymer NPs against spectra of the corresponding pure polymer NPs) reveals special interactions between the active agent and NP polymer matrix (Figure 3a and 3b).

Compared with the spectra of pure parabens, the spectral feature of loaded parabens is slightly changed.

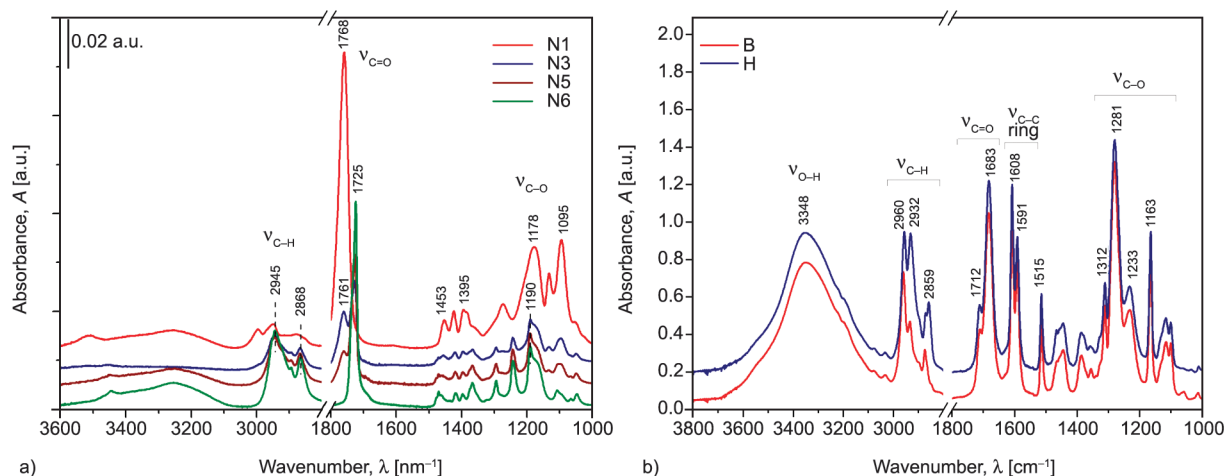


**Figure 2.** IR spectra of pure polymer nanoparticles (a), and butyl- (B) and hexyl- (H) parabens (b). For better visualization, spectra are shifted vertically. N signs the nanoparticles without paraben, while 1 to 6 the polymer composition (see Table 2).



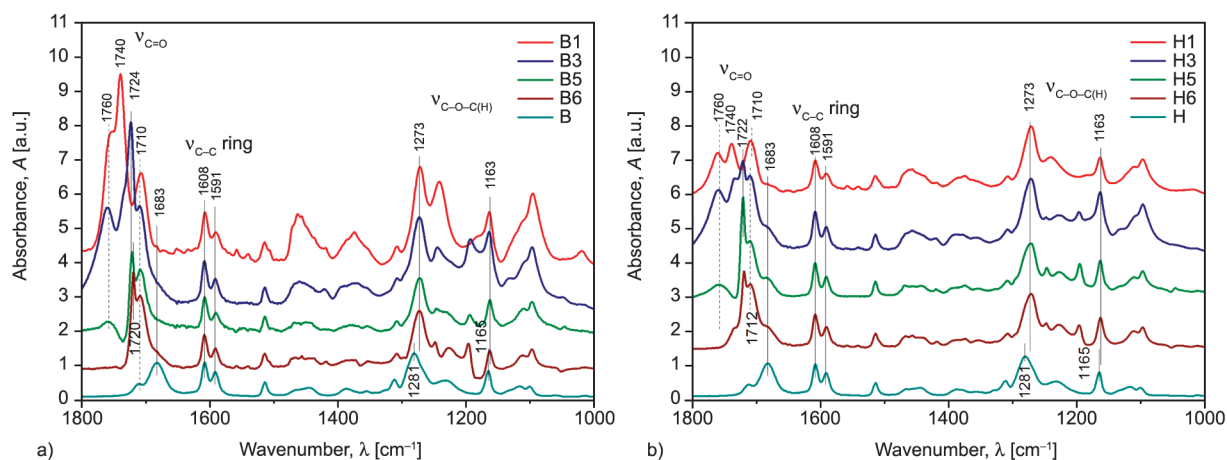


**Figure 3.** Difference spectra of butylparaben (a) and hexylparaben (b) loaded polymer nanoparticles (the appropriate spectrum of pure polymer is subtracted from the spectrum of the corresponding loaded polymer nanoparticle). For comparison, the spectrum of butylparaben (B) and that of hexylparaben (H) is also included. Spectra are normalized to the ring C–C stretching band intensity at  $1608\text{ cm}^{-1}$  and are shifted vertically for better visualization. 1 to 6 indicates the polymer composition (see Table 2).

The most spectacular difference is the lack (for butylparaben) or the significant suppression (for hexylparaben) of the band at  $1683\text{ cm}^{-1}$ . In parallel, the band at  $1710\text{ cm}^{-1}$ , assigned to intact carbonyl groups, is significantly increased. As the band at  $1683\text{ cm}^{-1}$  belongs to the  $\text{C}=\text{O}\dots\text{H}-\text{O}$  connectivity motif, it seems plausible that the encapsulated parabens are dissolved in the polymer matrix on a molecular level. This finding is further affirmed by the notable shift of C–O stretching vibration bands from  $1281$  to  $1279\text{ cm}^{-1}$  and from  $1165$  to  $1163\text{ cm}^{-1}$ . As to the hexylparaben (Figure 3b), however, a weak band (shoulder) of H-bonded  $\text{C}=\text{O}$  (at  $1683\text{ cm}^{-1}$ ) is still present, indicating the presence of a kind of

paraben ‘excess’. This is in line with the higher amount of loaded hexylparaben.

Regarding the structural changes in the polymer matrix, for both types of polymer, some new carbonyl bands are arising in the difference spectra. In the case of PLGA, two new carbonyl bands develop in the difference spectra: a shoulder at  $1760\text{ cm}^{-1}$  and a strong band  $1740\text{ cm}^{-1}$  (the carbonyl vibration band of pure PLGA appears at  $1768\text{ cm}^{-1}$ ). The significant shift towards lower wavenumbers suggests that the PLGA carbonyls are in H-bonding with parabens, presumably with their  $-\text{OH}$  groups. As to the PCL polymer, only a very narrow band at  $1724\text{ cm}^{-1}$  can be found in the difference spectra, with a moderate

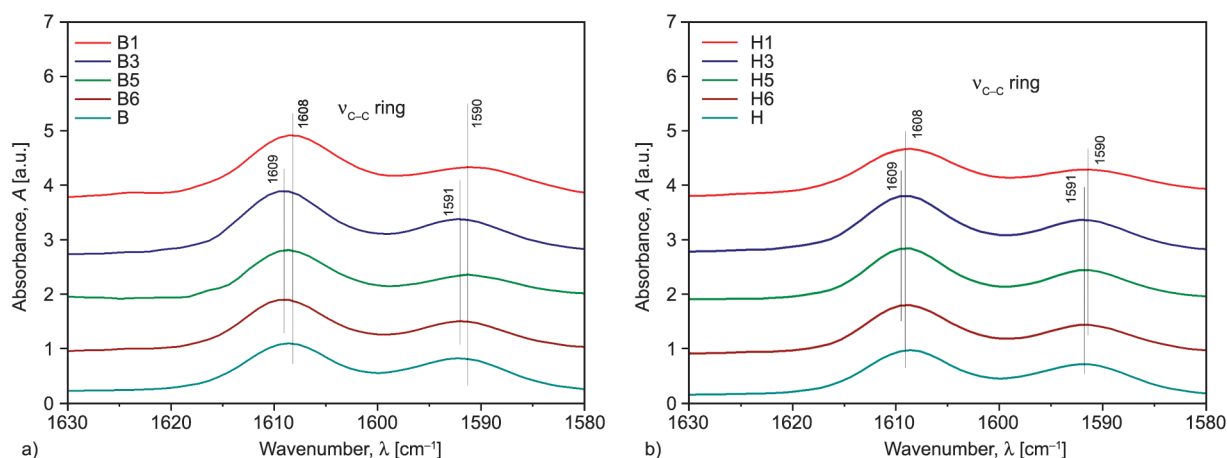


**Figure 4.** Ring C–C vibration spectral range of the difference spectra of butylparaben (a) and hexylparaben (b) loaded polymer nanoparticles (the appropriate spectrum of pure polymer is subtracted from the spectrum of the corresponding loaded polymer nanoparticle). For comparison, the spectrum of butylparaben (B) and that of hexylparaben (H) is also included. Spectra are shifted vertically for better visualization. 1 to 6 indicates the polymer composition (see Table 2).

shift (from 17251 to 1724  $\text{cm}^{-1}$ ). We speculate that, in this case, the  $-\text{CH}_2-$  moiety of the PCL might be involved in the interaction. The small spectral shifts in the ring C–C vibrations (Figure 4a and 4b) further confirm the difference between the PLGA – paraben, and PCL – paraben interaction, respectively.

For the PLGA-containing polymer matrix, the band at 1591  $\text{cm}^{-1}$  is slightly shifted to 1590  $\text{cm}^{-1}$ , while for PCL-based polymers the band at 1608  $\text{cm}^{-1}$  shifts towards 1609  $\text{cm}^{-1}$ . These small changes might be the consequence of different spatial locations of paraben molecules.

To sum up the results of IR spectroscopic investigation, we can state that both loaded parabens are dissolved on a molecular level. The hexylparaben loading is higher; however, a small amount of hexylparaben is still in interconnected form. The interaction sites of the two types of polymers (PLGA and PCL) are different, which may affect the paraben release in the case of PLGA-PCL mixed systems.

### 3.2.3. DSC analysis

DSC analysis of the pure polymers (N series) and all paraben-loaded systems (B and H series) were performed. (The polymer compositions are given in Table 2.)

Heating and cooling DSC curves for drug-free PLGA50, PCL and their blends are shown in Figure 5. The different character of PLGA50 (N1) and PCL (N6) is clearly demonstrated by the glass transition of PLGA50 and melting/crystallization of semicrystalline PCL. Those findings are in harmony with reported values for  $T_g$ : 42 °C [51] and  $T_m$ : 59–64 °C [52] for PLGA50 and PCL, respectively. The sign of crystallization can be discovered in all blends, which

**Table 6.** Peak temperatures of the melting peaks observed on the first heating DSC curves of the drug-free (N) and butyl- (B) or hexylparaben (H) loaded mixed polymer samples.

PCL ratio in the polymer matrix [w%]	$T_m^{1\text{st heating (N)}}$ [°C]	$T_m^{1\text{st heating (B)}}$ [°C]	$T_m^{1\text{st heating (H)}}$ [°C]
20	53.3	55.5	49.3
40	60.0	57.7	50.5
60	59.2	56.0	53.5
80	61.8	57.3	51.3

is more pronounced in systems with a higher PCL ratio. The peak melting temperatures for blend systems are tabulated in Table 6.

The DSC first heating and cooling curves are presented in Figure 6 for butylparaben and in Figure 7 for hexylparaben containing NP systems. All heating curves are characterized an endothermic peak in the range of 45–60 °C. The temperature of the corresponding exothermic peak in the cooling curves is below 25 °C.

Comparing the DSC curves of the pure (drug-free) and drug-loaded PLGA samples it can be concluded that both butyl- and hexylparaben drugs change the phase behaviour of PLGA. Interestingly, while pure PLGA (N1) shows only a glass transition with 42.6 °C glass transition temperature, the butyl- and hexylparaben-loaded PLGA samples (B1 and H1, respectively) show melting at 54.3 and 51.3 °C, respectively, during the first heating cycle. This observation indicates the formation of a mixed drug-PLGA crystalline phase in these samples. However, neither during the subsequent cooling cycle with the applied quite a high cooling rate (10 °C/min), nor on the second heating

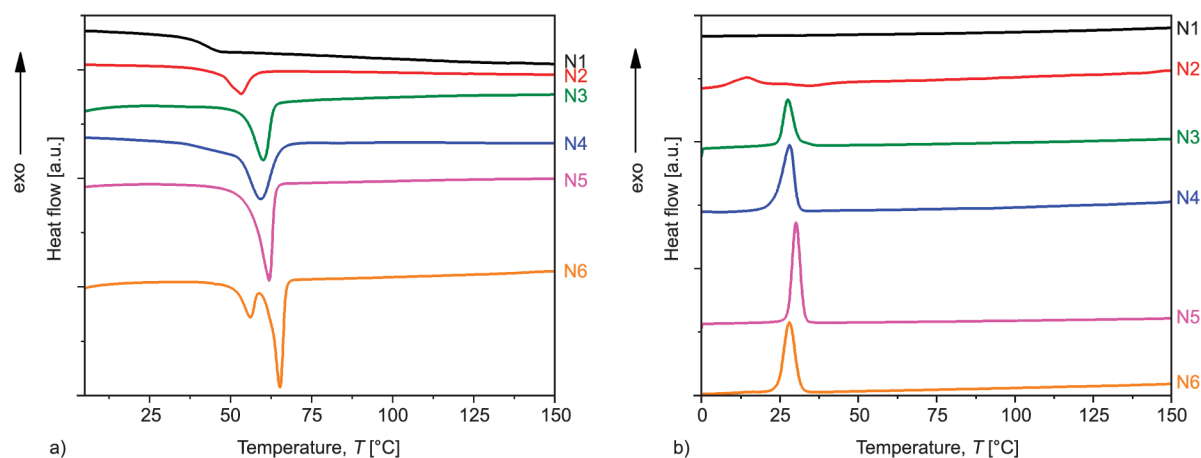


**Figure 5.** First heating (a) and cooling (b) DSC curves of the drug-free polymers and polymer mixtures. 1 to 6 is the polymer composition (see Table 2).

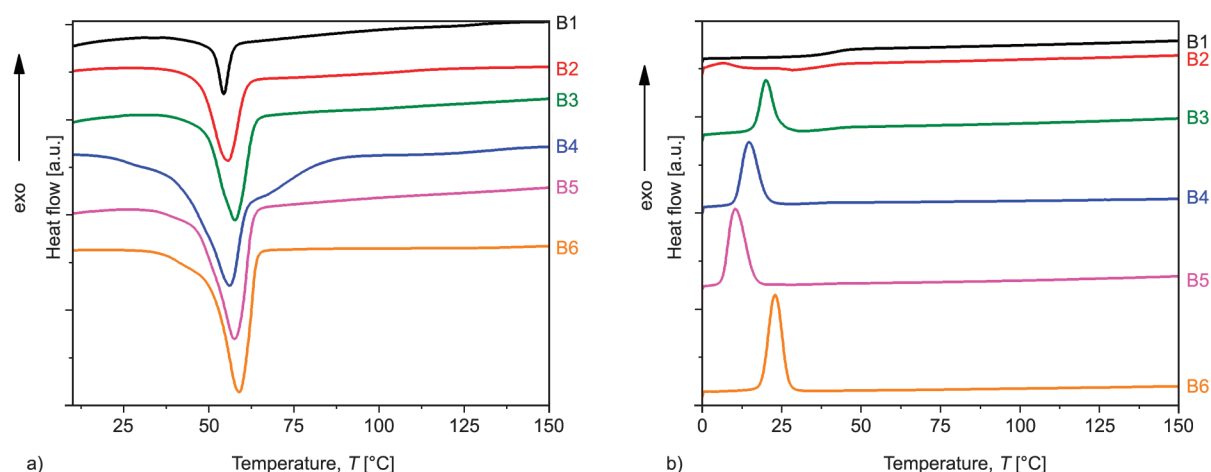


**Figure 6.** First heating (a) and cooling (b) DSC curves of the butylparaben-loaded polymers and polymer mixtures. 1 to 6 is the polymer composition (see Table 2).

curve (not shown) crystallization/melting peaks cannot be seen which indicates the slow forming rate of the mixed crystals.

In the case of PCL, on the first heating curve of the pure polymer, two melting points (56.0 and 65.2 °C, N6) can be seen according to former reported results [53]. However, in the loaded case, only one melting peak (59.0 °C for the butyl and 55.8 °C for the hexyl drug case, B6 and H6, respectively) can be observed on the first heating curves indicating the change of the crystal morphology due to drug-polymer interaction in the presence of the drug. In the polymer blend cases, melting appears in the first heating cycle while crystallization in the cooling cycle for the drug-free and the loaded samples, too. However, considering the peak temperatures of the first heating (Table 6) it can be stated that there is a shift for the loaded samples which is higher in the presence of the hexylparaben. This also indicates the mixing of

the parabens with the polymer matrix, which is also proved by the absence of the melting peak of the butylparaben at 69 °C on the first heating curves of the loaded samples. (Hexylparaben melts at 53 °C, so its melting would overlap with the melting of the PCL). Additionally, on the cooling curves of the loaded samples with high PLGA content, a glass transition can also be observed, indicating the presence of phase separation in the loaded samples, which is proved by the second heating curves (not shown), too.

### 3.2.4. Kinetics of drug release

Drug release profiles have been determined for the paraben-loaded PLGA50, PCL and their blend NPs. The amount of released drugs relative to the total drug content of the particles as a function of time is presented in Figure 8. The relative amount of released butylparaben is higher compared to hexylparaben in

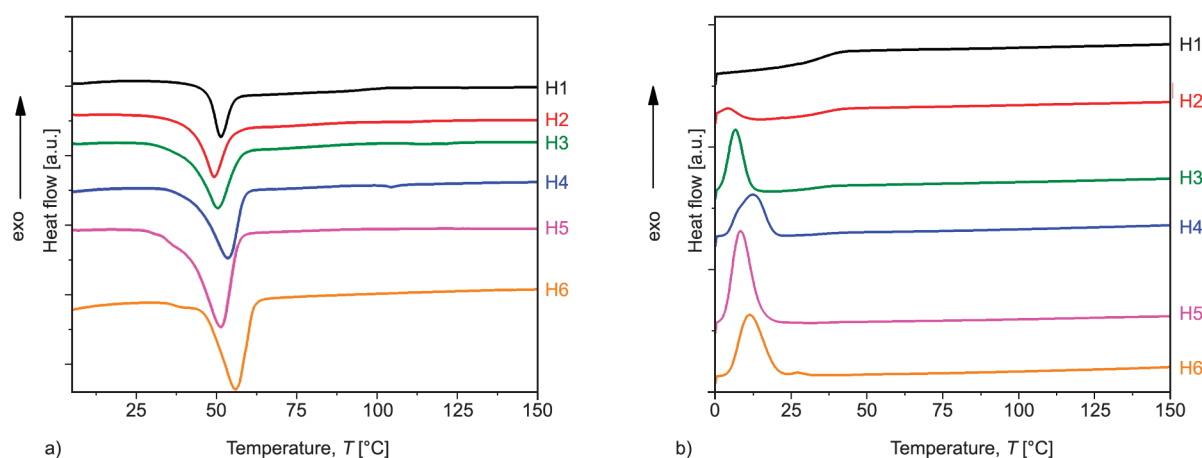


**Figure 7.** First heating (a) and cooling (b) DSC curves of the hexylparaben-loaded polymers and polymer mixtures. 1 to 6 is the polymer composition (see Table 2).

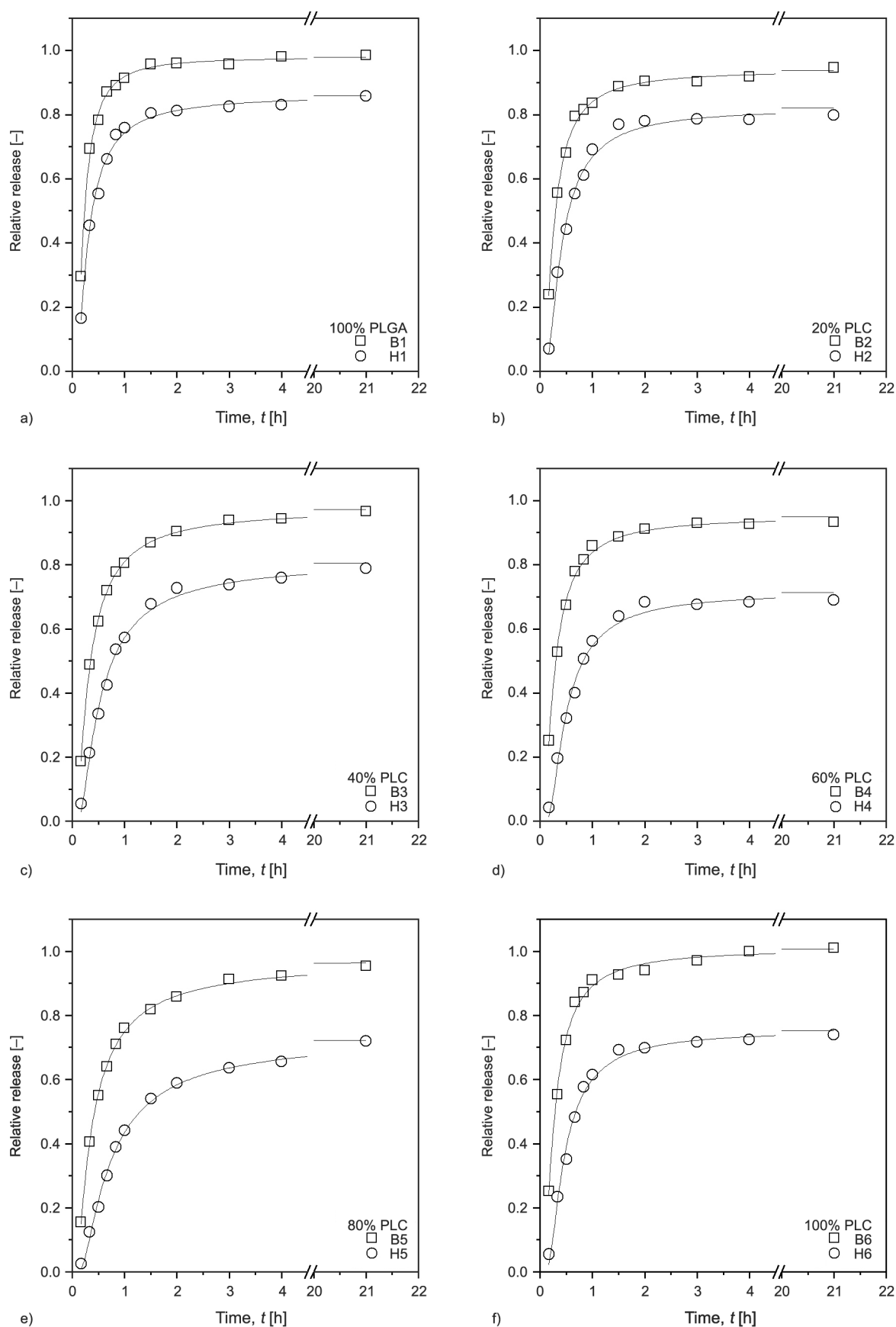


**Figure 8.** Relative release ratio profiles of butylparaben (B) and hexylparaben (H) from various polymer NPs: PLGA50 (a), PLGA50-PCL blends with 20% PCL (b), 40% PCL (c), 60% PCL (d), 80% PCL (e) and PCL (f) nanoparticles. Continuous lines represent the fitted Gompertz model.



all NP systems. Almost 100% of butylparaben is released from PLGA50 and PCL NPs within 21 hours. The cumulative released amount, however is somewhat lower for the blend systems being in the range of 93–96%. The released amount of hexylparaben was found to be considerably lower both from pure polymers and blend NPs during the time interval investigated. The difference which is appr. 12% for PLGA50 is increasing with PCL content up to 27%, indicating the retard effect of PCL probably by the favourable interaction between the hydrophobic matrix and the hexylparaben. Similar behaviour is observed if we compare the time needed to release 50% of the paraben encapsulated. The release of 50% butylparaben occurs in about 1 min, while this time is doubled by applying blend NPs. For hexylparaben the corresponding ‘half-life’ for PLGA50 is 23 min, which could be more than tripled using blend system no. 5. Experimental models developed for describing drug release kinetic provide a more specific evaluation. The Gompertz model is a simple exponential model suitable for burst release profiles where the released drug amount converges to a maximum value. A reasonably good fitting obtained is shown in Figure 8 and Table 7. A significant difference between the two drug formulations is the maximum released drug ratio which is represented in the model by the  $C_{\max}$  parameter. Although the model cannot be used to infer the release mechanism, the values of the  $b$  constants can be used to compare release rates, where the greater the absolute value of  $b$ , the faster the release. For both parabens, similar tendencies can be observed. The rate is highest for PLGA50 and PCL

NPs while generally lower for blend systems, especially for no. 5 with 80% PCL content.

To gain some insight into the mechanism of drug release the experimental profiles have been fitted with the Korsmeyer-Peppas model. For spherical particles, if  $n < 0.43$ , the mechanism can be considered quasi-Fickian diffusion-controlled ( $n = 0.43$  corresponds to Fickian diffusion) where the rate of release is mostly dependent on the diffusion of the drug in the polymer matrix. For  $n \geq 0.85$  the release mechanism is suggested to be governed by case II transport. This type of release is mainly associated with polymers in a glassy state where the outer layers are swollen by the medium. With the progression of the swelling front, relaxation processes occur in the polymer matrix leading to the release of the encapsulated drug. When  $0.43 < n < 0.85$ , the release rate is governed by diffusion and case II mechanisms [54].

Based on the Korsmeyer-Peppas model, samples had their release exponent,  $n$  values between 0.45 and 0.85, indicating a release mechanism where swelling-induced relaxations and drug diffusions are occurring concurrently. Since the values are closer to 0.85, it can be assumed the swelling governed relaxation processes are dominant. It should be noted that for both the butyl- and hexylparaben formulations, the  $n$  values have a maximum of 80% PCL polymer composition. For the hexylparaben samples, the  $n$  values are increased, indicating a more pronounced case II type mechanism in the initial release profile. Considering the rate of release ( $k_m$ ) the values for blend systems (except H2) are lower compared to PLGA50 or PCL. This result might be related to retard effect

**Table 7.** Fitted parameters of the Gompertz and Korsmeyer-Peppas release models.

PCL [%]	Sample	Gompertz				Korsmeyer-Peppas		
		$C_{\max}$ [–]	$a$ [–]	$b$ [–]	$R^2$ [–]	$k_m$ [h <sup>–n</sup> ]	$n$ [–]	$R^2$ [–]
0	B1	0.98±0.01	0.06±0.01	–1.63±0.07	0.996	1.41±0.43	0.77±0.31	0.903
20	B2	0.94±0.01	0.11±0.01	–1.40±0.05	0.997	1.11±0.12	0.74±0.14	0.953
40	B3	0.98±0.01	0.19±0.01	–1.21±0.02	0.999	1.04±0.13	0.80±0.17	0.947
60	B4	0.95±0.01	0.13±0.01	–1.34±0.06	0.996	1.08±0.09	0.73±0.11	0.971
80	B5	0.97±0.01	0.26±0.01	–1.10±0.03	0.999	0.95±0.11	0.86±0.16	0.961
100	B6	1.01±0.01	0.12±0.01	–1.37±0.08	0.994	1.18±0.11	0.77±0.11	0.972
0	H1	0.86±0.01	0.15±0.02	–1.36±0.08	0.994	0.88±0.07	0.72±0.13	0.947
20	H2	0.82±0.02	0.21±0.03	–1.44±0.11	0.992	0.72±0.03	0.72±0.08	0.982
40	H3	0.81±0.02	0.35±0.03	–1.26±0.09	0.994	0.59±0.02	0.86±0.08	0.981
60	H4	0.72±0.02	0.27±0.04	–1.49±0.15	0.990	0.58±0.01	0.90±0.07	0.988
80	H5	0.73±0.01	0.52±0.03	–1.19±0.06	0.997	0.45±0.02	1.07±0.12	0.981
100	H6	0.75±0.02	0.23±0.03	–1.52±0.13	0.992	0.64±0.02	0.84±0.09	0.974

of blend structure.  $k_m$  has a minimum for the 80% PCL polymer for both formulations.

Based on these findings, it can be estimated that the core of the polymer particles is in a non-hydrated state alongside the aqueous medium, slowly penetrating into the matrix. Even though both polymers are considered hydrophobic ones, it is well known that a limited swelling by water can occur [21, 22, 55–58].

To quantify the contributions of the diffusion and relaxation governed transports in the release mechanism, the data were also fitted with the Peppas-Sahlin model. It was found that in all cases, the  $k_2$  values were significantly higher than the  $k_1$  values indicating the dominance of the case II transport mechanism. Although the poor fitting did not allow for finding distinct tendencies for the different formulations, it was confirmed that the release is governed/slowed down by the polymer relaxation processes in blend systems.

It is worth considering not only the release ratio [%] but the amount of active component released from a given volume of NP formula during the time interval investigated. The cumulative released amount of parabens from 1 ml NP sample as a function of time are displayed in Figure 9 for three selected polymer matrices, the pure PLGA50 (1), PCL (6) and a blended system with 20% PLGA content (5).

The dual influence of the polymer matrix can be observed. Changing the PLGA50 to PCL or PCL blend results in highly enhanced drug loading and elevated release in the first three hours as well. The released

amount of butylparaben approaches 0.05 mg, compared to PLGA50 system presenting 0.025 mg. A similar value of hexylparaben exceeds 0.1 mg related to 0.04 mg in the case of PLGA50. That demonstrates that the proper choice of the polymer matrix for the bioactive compound allows remarkably increased encapsulation and release efficiency.

The other aspect is the release kinetic, which is also affected by the polymer composition of the NP as it was analysed using the experimental kinetic models. The cumulative released amount quickly reaches a steady value within one hour for systems B1, H1 and B6. On the contrary to that, the release is more gradual and further increases even after 3 hours for blends B5 and especially for H5. That slower, more elongated release which was also presented by Korsmeyer-Peppas model (Table 7) might be related to the special structure of the PLGA50-PCL blend. According to the DSC measurements, the polymer mixture is supposed to form a phase-separated system (Figure 5, Table 6). This immiscible (or poorly miscible) behaviour was previously found for drug carrier PLGA50 and PCL films [59] and nanofibres [7]. The possible presence of separated domains and extended inner interface in the NPs presumably slow down the migration of paraben molecules. This effect is expected to be more pronounced for the less mobile hexylparaben as it is shown by data in Figure 9. Furthermore, it was stated that when the weight fraction of one component is reduced considerably (below 25%), it is expected that the minor component will assume the forms of isolated islets within the major phase [59]. The lost interconnectivity of the minor phase might lead to reduced release. That structural property might be the reason for the slowest release rate obtained for system 5 with 20% of PLGA50 in PCL.

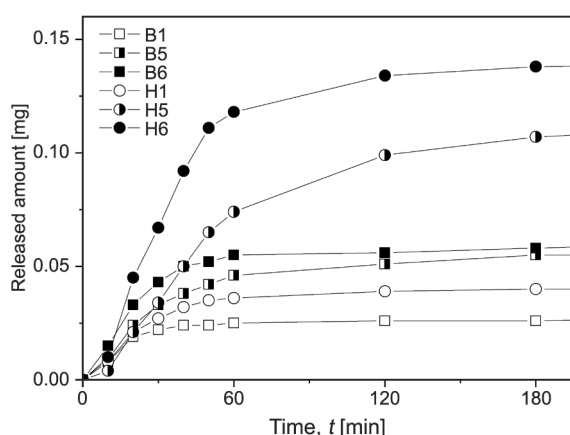


**Figure 9.** The cumulative released amount of butyl- (B) and hexylparabens (H) from 1 ml of various NP systems: PLGA50 (1), PCL (6) and PLGA50-PCL blend (5). 1, 5, 6 are the polymer compositions (see Table 2).

#### 4. Conclusions

The proper match of the polarity of encapsulation matrix and coprecipitating drug in the nanoprecipitation process is beneficial to achieve high drug content of the carrier. It is worth to make an effort to accomplish this matching as the experimental investigation using model drugs and different matrix polymers demonstrated here. Both sides should be considered for the sake of success since the polarity of the bioactive molecule can be tuned by conjugation with alkyl chains, while the appropriate selection of the matrix polymer can also contribute to the preparation of a drug delivery system with high loading.

The composition of the carrier polyester was varied, and its effect on the encapsulation was tested. There was no significant difference when PLGA50 or PLGA75 were used for encapsulation, whereas applying the most hydrophobic PCL the amount of paraben in NPs was multiplied. To finely control the pharmaceutical behaviour of the NPs system, blending of PLGA50 and PCL was introduced in the nanoprecipitation. The nanoprecipitation process using these two polymers together resulted in blend NPs with considerable and predictable drug loading. Furthermore, the release kinetic can also be influenced by the blending of matrix polymers, leading to a notable reduction in release rate.

## Acknowledgements

This work was supported by OTKA K 131594, National Research Development and Innovation Office, Hungary and Lendület (Momentum) Program of the Hungarian Academy of Sciences. This work was completed in the ELTE Thematic Excellence Program (SZINT+) supported by the Hungarian Ministry for Innovation and Technology and VEKOP-2.3.2-16-2017-00014 supported by National Research Development and Innovation Office, Hungary. Project no. 2018-1.2.1-NKP-2018-00005 was implemented with the support provided by the National Research, Development and Innovation Fund of Hungary, financed under the 2018-1.2.1-NKP funding scheme.

Laura Nagyné Bereczki's help (Plasma Chemistry Research Group, Institute of Materials and Environmental Chemistry, Research Centre for Natural Sciences) during the DSC measurements is acknowledged.

## References

- [1] Ciobanu M., Heurtault B., Schultz P., Ruhlmann C., Muller C. D., Frisch B.: Layersome: Development and optimization of stable liposomes as drug delivery system. *International Journal of Pharmaceutics*, **344**, 154–157 (2007).  
<https://doi.org/10.1016/j.ijpharm.2007.05.037>
- [2] Gidwani B., Vyas A.: A comprehensive review on cyclodextrin-based carriers for delivery of chemotherapeutic cytotoxic anticancer drugs. *BioMed Research International*, **2015**, 198268 (2015).  
<https://doi.org/10.1155/2015/198268>
- [3] Nagy N. Zs., Varga Z., Mihály J., Domján A., Fenyvesi É., Kiss É.: Highly enhanced curcumin delivery applying association type nanostructures of block copolymers, cyclodextrins and polycyclodextrins. *Polymers*, **12**, 2167 (2020).  
<https://doi.org/10.3390/polym12092167>
- [4] Kiss É., Schnöller D., Pribranská K., Hill K., Péntes Cs. B., Horváti K., Bösze Sz.: Nanoencapsulation of antitubercular drug isoniazid and its lipopeptide conjugate. *Journal of Dispersion Science and Technology*, **32**, 1728–1734 (2011).  
<https://doi.org/10.1080/01932691.2011.616128>
- [5] Kasza G., Gyulai G., Ábrahám Á., Szarka G., Iván B., Kiss É.: Amphiphilic hyperbranched polyglycerols in a new role as highly efficient multifunctional surface active stabilizers for poly(lactic/glycolic acid) nanoparticles. *RSC Advances*, **7**, 4348–4352 (2017).  
<https://doi.org/10.1039/C6RA27843D>
- [6] Carson D., Jiang Y., Woodrow K. A.: Tunable release of multiclass anti-HIV drugs that are water-soluble and loaded at high drug content in polyester blended electrospun fibers. *Pharmaceutical Research*, **33**, 125–136 (2016).  
<https://doi.org/10.1007/s11095-015-1769-0>
- [7] Contreras A., Raxworthy M. J., Wood S., Tronci G.: Hydrolytic degradability, cell tolerance and on-demand antibacterial effect of electrospun photodynamically active fibres. *Pharmaceutics*, **12**, 711 (2020).  
<https://doi.org/10.3390/pharmaceutics12080711>
- [8] Farkas B., Balogh A., Farkas A., Marosi G., Nagy Zs. K.: Frequency and waveform dependence of alternating current electrospinning and their uses for drug dissolution enhancement. *International Journal of Pharmaceutics*, **586**, 119593 (2020).  
<https://doi.org/10.1016/j.ijpharm.2020.119593>
- [9] Yata V. K., Ranjan S., Dasgupta N., Lichtfouse E.: *Nanopharmaceuticals: Principles and applications*, Vol. 1. Springer, Cham (2021).
- [10] Bruschi M. L.: Drug delivery systems. in 'Strategies to modify the drug release from pharmaceutical systems' (ed.: Bruschi M. L.) Woodhead, Amsterdam, 87–194 (2015).  
<https://doi.org/10.1016/B978-0-08-100092-2.00006-0>
- [11] Mota A. H., Santos-Rebello A., Almeida A. J., Reis C. P.: Therapeutic implications of nanopharmaceuticals in skin delivery. in 'Nanopharmaceuticals: Principles and applications' (eds.: Yata V. K., Ranjan S., Dasgupta N., Lichtfouse E.) Springer International Publishing, Cham, Vol. 1. 205–272 (2021).  
[https://doi.org/10.1007/978-3-030-44925-4\\_6](https://doi.org/10.1007/978-3-030-44925-4_6)
- [12] Danhier F., Ansorena E., Silva J. M., Coco R., le Breton A., Préat V.: PLGA-based nanoparticles: An overview of biomedical applications. *Journal of Controlled Release*, **161**, 505–522 (2012).  
<https://doi.org/10.1016/j.jconrel.2012.01.043>
- [13] Kiss É., Gyulai G., Péntes Cs. B., Idei M., Horváti K., Bacsa B., Bösze Sz.: Tuneable surface modification of PLGA nanoparticles carrying new antitubercular drug candidate. *Colloids and Surfaces A: Physicochemical and Engineering Aspects*, **458**, 178–186 (2014).  
<https://doi.org/10.1016/j.colsurfa.2014.05.048>

- [14] Horváti K., Bacsá B., Kiss É., Gyulai G., Fodor K., Balka G., Rusvai M., Szabó E., Hudecz F., Bősze Sz.: Nanoparticle encapsulated lipopeptide conjugate of antitubercular drug isoniazid: *In vitro* intracellular activity and *in vivo* efficacy in a guinea pig model of tuberculosis. *Bioconjugate Chemistry*, **25**, 2260–2268 (2014). <https://doi.org/10.1021/bc500476x>
- [15] Salama A. H., Mahmoud A. A., Kamel R.: A novel method for preparing surface-modified fluocinolone acetonide loaded PLGA nanoparticles for ocular use: *In vitro* and *in vivo* evaluations. *AAPS PharmSciTech*, **17**, 1159–1172 (2016). <https://doi.org/10.1208/s12249-015-0448-0>
- [16] El-Hammadi M. M., Arias J. L.: Recent advances in the surface functionalization of PLGA-based nanomedicines. *Nanomaterials*, **12**, 354 (2022). <https://doi.org/10.3390/nano12030354>
- [17] Varga N., Turcsányi Á., Hornok V., Csapó E.: Vitamin E-loaded PLA- and PLGA-based core-shell nanoparticles: Synthesis, structure optimization and controlled drug release. *Pharmaceutics*, **11**, 357 (2019). <https://doi.org/10.3390/pharmaceutics11070357>
- [18] Gyulai G., Péntes Cs. B., Mohai M., Csempesz F., Kiss É.: Influence of surface properties of polymeric nanoparticles on their membrane affinity. *European Polymer Journal*, **49**, 2495–2503 (2013). <https://doi.org/10.1016/j.eurpolymj.2013.02.024>
- [19] Gyulai G., Magyar A., Rohonczy J., Orosz J., Yamasaki M., Bősze Sz., Kiss É.: Preparation and characterization of cationic Pluronic for surface modification and functionalization of polymeric drug delivery nanoparticles. *Express Polymer Letters*, **10**, 216–226 (2016). <https://doi.org/10.3144/expresspolymlett.2016.20>
- [20] Kim J. Y., Cho D-W.: Blended PCL/PLGA scaffold fabrication using multi-head deposition system. *Microelectronic Engineering*, **86**, 1447–1450 (2009). <https://doi.org/10.1016/j.mee.2008.11.026>
- [21] Li Q., Wang Z., Zhao Q., Wang L., Wang S., Kong D.: Tissue engineering scaffold electrospun from poly( $\epsilon$ -caprolactone)-*b*-poly(sulfobetaine methacrylate) block copolymers with improved hydrophilicity and good cytocompatibility. *e-Polymers*, **12**, no.050 (2012). <https://doi.org/10.1515/epoly.2012.12.1.584>
- [22] Jonnalagadda J. B., Rivero I. V., Warzywoda J.: *In-vitro* degradation characteristics of poly( $\epsilon$ -caprolactone)/poly(glycolic acid) scaffolds fabricated via solid-state cryomilling. *Journal of Biomaterials Applications*, **30**, 472–483 (2015). <https://doi.org/10.1177/0885328215592853>
- [23] Pawlik J., Łukowicz K., Cholewa-Kowalska K., Osyczka A. M.: New insights into the PLGA and PCL blending: Physico-mechanical properties and cell response. *Materials Research Express*, **6**, 085344 (2019). <https://doi.org/10.1088/2053-1591/ab2823>
- [24] Varan C., Bilensoy E.: Cationic PEGylated polycaprolactone nanoparticles carrying post-operation docetaxel for glioma treatment. *Beilstein Journal of Nanotechnology*, **8**, 1446–1456 (2017). <https://doi.org/10.3762/bjnano.8.144>
- [25] Snehathatha M., Venugopal K., Saha R. N.: Etoposide-loaded PLGA and PCL nanoparticles I: Preparation and effect of formulation variables. *Drug Delivery*, **15**, 267–275 (2008). <https://doi.org/10.1080/10717540802174662>
- [26] Chang S. H., Lee H. J., Park S., Kim Y., Jeong B.: Fast degradable polycaprolactone for drug delivery. *Biomacromolecules*, **19**, 2302–2307 (2018). <https://doi.org/10.1021/acs.biomac.8b00266>
- [27] Nagy N. Zs., Varga Z., Mihály J., Kasza Gy., Iván B., Kiss É.: Highly efficient encapsulation of curcumin into and pH-controlled drug release from poly( $\epsilon$ -caprolactone) nanoparticles stabilized with a novel amphiphilic hyperbranched polyglycerol. *Express Polymer Letters*, **14**, 90–101 (2020). <https://doi.org/10.3144/expresspolymlett.2020.8>
- [28] Rahman M. A., Yusuf M., Alshammari T., Faiyazuddin M.: Nanopharmaceuticals: In relevance to drug delivery and targeting, in ‘Nanopharmaceuticals: Principles and applications’ (eds.: Yata V. K., Ranjan S., Dasgupta N., Lichtfouse E.) Springer, Cham, Vol. 2, 77–112 (2021). [https://doi.org/10.1007/978-3-030-44921-6\\_3](https://doi.org/10.1007/978-3-030-44921-6_3)
- [29] Pozsgay J., Babos F., Uray K., Magyar A., Gyulai G., Kiss É., Nagy Gy., Rojkovich B., Hudecz F., Sármay G.: *In vitro* eradication of citrullinated protein specific B-lymphocytes of rheumatoid arthritis patients by targeted bifunctional nanoparticles. *Arthritis Research and Therapy*, **18**, 15 (2016). <https://doi.org/10.1186/s13075-016-0918-0>
- [30] Fessi H., Puisieux F., Devissaguet J. Ph., Ammoury N., Benita S.: Nanocapsule formation by interfacial polymer deposition following solvent displacement. *International Journal of Pharmaceutics*, **55**, R1–R4 (1989). [https://doi.org/10.1016/0378-5173\(89\)90281-0](https://doi.org/10.1016/0378-5173(89)90281-0)
- [31] Hrkach J., von Hoff D., Ali M. M., Andrianova E., Auer J., Campbell T., de Witt D., Figa M., Figueiredo M., Horhota A., Low S., McDonnell K., Peeke E., Retnarajan B., Sabnis A., Schnipper E., Song J. J., Song Y. H., Summa J., Tompsett D., Troiano G., van Geen Hoven T., Wright J., LoRusso P., Kantoff P. W., Bander N. H., Sweeney C., Farokhzad O. C., Langer R., Zale S.: Pre-clinical development and clinical translation of a PSMA-targeted docetaxel nanoparticle with a differentiated pharmacological profile. *Science Translational Medicine*, **4**, 128ra39 (2012). <https://doi.org/10.1126/scitranslmed.3003651>
- [32] Liu Y., Yang G., Baby T., Tengjisi, Chen D., Weitz D. A., Zhao C-X.: Stable polymer nanoparticles with exceptionally high drug loading by sequential nanoprecipitation. *Angewandte Chemie International Edition*, **59**, 4720–4728 (2020). <https://doi.org/10.1002/anie.201913539>



- [33] Soni M. G., Carabin I. G., Burdock G. A.: Safety assessment of esters of p-hydroxybenzoic acid (parabens). *Food and Chemical Toxicology*, **43**, 985–1015 (2005).  
<https://doi.org/10.1016/j.fct.2005.01.020>
- [34] Flasiński M., Kowal S., Broniatowski M., Wydro P.: Influence of parabens on bacteria and fungi cellular membranes: Studies in model two-dimensional lipid systems. *Journal of Physical Chemistry B*, **122**, 2332–2340 (2018).  
<https://doi.org/10.1021/acs.jpcb.7b10152>
- [35] TOXNET Toxicology Data Network, U.S. National Library of Medicine Available online:  
<https://chem.nlm.nih.gov/chemidplus>  
(accessed on Feb.10, 2022).
- [36] Mande P. P., Bachhav S. S., Devarajan P. V.: Bioenhanced advanced third generation solid dispersion of tadalafil: Repurposing with improved therapy in pyelonephritis. *Asian Journal of Pharmaceutical Sciences*, **12**, 569–579 (2017).  
<https://doi.org/10.1016/j.ajps.2017.07.001>
- [37] Krause S.: Polymer–polymer compatibility. in ‘Polymer blends’ (eds.: Paul D. R., Newman S.) Academic Press Incorporation, London, 15–113 (1978).  
<https://doi.org/10.1016/B978-0-12-546801-5.50008-6>
- [38] Hansen C. M.: Hansen solubility parameters: A user’s handbook. CRC Press, Boca Raton (2007).
- [39] Kitak T., Dumičić A., Planinšek O., Šibanc R., Srčić S.: Determination of solubility parameters of ibuprofen and ibuprofen lysinate. *Molecules*, **20**, 21549–21568 (2015).  
<https://doi.org/10.3390/molecules201219777>
- [40] Dash S., Murthy P. N., Nath L., Chowdhury P.: Kinetic modeling on drug release from controlled drug delivery systems. *Acta Poloniae Pharmaceutica*, **67**, 217–223 (2010).
- [41] Korsmeyer R. W., Gurny R., Doelker E., Buri P., Peppas N. A.: Mechanisms of solute release from porous hydrophilic polymers. *International Journal of Pharmaceutics*, **15**, 25–35 (1983).  
[https://doi.org/10.1016/0378-5173\(83\)90064-9](https://doi.org/10.1016/0378-5173(83)90064-9)
- [42] Peppas N. A., Sahlin J. J.: A simple equation for the description of solute release. III. Coupling of diffusion and relaxation. *International Journal of Pharmaceutics*, **57**, 169–172 (1989).  
[https://doi.org/10.1016/0378-5173\(89\)90306-2](https://doi.org/10.1016/0378-5173(89)90306-2)
- [43] Tóth T., Kiss É.: A method for the prediction of drug content of poly(lactic-co-glycolic)acid drug carrier nanoparticles obtained by nanoprecipitation. *Journal of Drug Delivery Science and Technology*, **50**, 42–47 (2019).  
<https://doi.org/10.1016/j.jddst.2019.01.010>
- [44] Mora-Huertas C. E., Fessi H., Elaissari A.: Polymer-based nanocapsules for drug delivery. *International Journal of Pharmaceutics*, **385**, 113–142 (2010).  
<https://doi.org/10.1016/j.ijpharm.2009.10.018>
- [45] Tavares M. R., de Menezes L. R., Dutra Filho J. C., Cabral L. M., Tavares M. I. B.: Surface-coated polycaprolactone nanoparticles with pharmaceutical application: Structural and molecular mobility evaluation by TD-NMR. *Polymer Testing*, **60**, 39–48 (2017).  
<https://doi.org/10.1016/j.polymertesting.2017.01.032>
- [46] Kiss É., Bertóti I., Vargha-Butler E. I.: XPS and wettability characterization of modified poly(lactic acid) and poly(lactic/glycolic acid) films. *Journal of Colloid and Interface Science*, **245**, 91–98 (2002).  
<https://doi.org/10.1006/jcis.2001.7954>
- [47] Bordes C., Fréville V., Ruffin E., Marote P., Gauvrit J. Y., Briançon S., Lantéri P.: Determination of poly( $\epsilon$ -caprolactone) solubility parameters: Application to solvent substitution in a microencapsulation process. *International Journal of Pharmaceutics*, **383**, 236–243 (2010).  
<https://doi.org/10.1016/j.ijpharm.2009.09.023>
- [48] Schenderlein S., Lück M., Müller B. W.: Partial solubility parameters of poly(D,L-lactide-co-glycolide). *International Journal of Pharmaceutics*, **286**, 19–26 (2004).  
<https://doi.org/10.1016/j.ijpharm.2004.07.034>
- [49] Phillipson K., Hay J. N., Jenkins M. J.: Thermal analysis FTIR spectroscopy of poly( $\epsilon$ -caprolactone). *Thermochimica Acta*, **595**, 74–82 (2014).  
<https://doi.org/10.1016/j.tca.2014.08.027>
- [50] Gelbrich T., Braun D. E., Ellern A., Griesser U. J.: Four polymorphs of methyl paraben: Structural relationships and relative energy differences. *Crystal Growth and Design*, **13**, 1206–1217 (2013).  
<https://doi.org/10.1021/cg301639r>
- [51] Barbanti S. H., Santos A. R., Zavaglia C. A. C., Duek E. A. R.: Poly( $\epsilon$ -caprolactone) and poly(D,L-lactic acid-co-glycolic acid) scaffolds used in bone tissue engineering prepared by melt compression–particulate leaching method. *Journal of Materials Science: Materials in Medicine*, **22**, 2377 (2011).  
<https://doi.org/10.1007/s10856-011-4398-0>
- [52] Cameron R. E., Kamvari-Moghaddam A.: Synthetic bioresorbable polymers. in ‘Durability and reliability of medical polymers’ (eds.: Jenkins M., Stamboulis A.) Woodhead Publishing, Cambridge, 96–118 (2012).  
<https://doi.org/10.1533/9780857096517.1.96>
- [53] Groeninckx G., Vanneste M., Everaert V.: Crystallization, morphological structure, and melting of polymer blends. in ‘Polymer blends handbook’ (ed.: Utracki L. A.) Springer, Dordrecht, 203–294 (2003).  
[https://doi.org/10.1007/0-306-48244-4\\_3](https://doi.org/10.1007/0-306-48244-4_3)
- [54] Ritger P. L., Peppas N. A.: A simple equation for description of solute release II. Fickian and anomalous release from swellable devices. *Journal of Controlled Release*, **5**, 37–42 (1987).  
[https://doi.org/10.1016/0168-3659\(87\)90035-6](https://doi.org/10.1016/0168-3659(87)90035-6)

- [55] Kiss É., Takács M. G., Bertóti I., Vargha-Butler E. I.: Surface properties of poly(lactic/glycolic acid)-Pluronic® blend films. *Polymers for Advanced Technologies*, **14**, 839–846 (2003).  
<https://doi.org/10.1002/pat.404>
- [56] Gyulai G., Péntes Cs. B., Mohai M., Lohner T., Petrik P., Kurunczi S., Kiss É.: Interfacial properties of hydrophilized poly(lactic-co-glycolic acid) layers with various thicknesses. *Journal of Colloid and Interface Science*, **362**, 600–606 (2011).  
<https://doi.org/10.1016/j.jcis.2011.06.055>
- [57] Bulatović V. O., Mandić V., Kučić Grgić D., Ivančić A.: Biodegradable polymer blends based on thermoplastic starch. *Journal of Polymers and the Environment*, **29**, 492–508 (2021).  
<https://doi.org/10.1007/s10924-020-01874-w>
- [58] Hedayati S. K., Behraves A. H., Hasannia S., Kordi O., Pourghaumi M., Saed A. B., Gashtasbi F.: Additive manufacture of PCL/nHA scaffolds reinforced with biodegradable continuous fibers: Mechanical properties, *in-vitro* degradation profile, and cell study. *European Polymer Journal*, **162**, 110876 (2022).  
<https://doi.org/10.1016/j.eurpolymj.2021.110876>
- [59] Lao L. L., Venkatraman S. S., Peppas N. A.: Modeling of drug release from biodegradable polymer blends. *European Journal of Pharmaceutics and Biopharmaceutics*, **70**, 796–803 (2008).  
<https://doi.org/10.1016/j.ejpb.2008.05.024>